DR CEM YAMALI (Orcid ID : 0000-0002-4833-7900)

Article type : Research Article

Synthesis, molecular modeling and biological evaluation of 4-[5-aryl-3-(thiophen-2-yl)-4,5-dihydro-1*H*-pyrazol-1-yl] benzenesulfonamides towards acetylcholinesterase, carbonic anhydrase I and II enzymes

Cem Yamali[1], Halise Inci Gul[1*], Abdulilah Ece[2], Parham Taslimi[3], Ilhami Gulcin[3]

[1]Department of Pharmaceutical Chemistry, Faculty of Pharmacy, Ataturk University, Erzurum, 25040, Turkey
[2]Department of Pharmaceutical Chemistry, Faculty of Pharmacy, Biruni University, Istanbul, 34010, Turkey
[3]Department of Chemistry, Faculty of Arts and Sciences, Ataturk University, Erzurum, 25040, Turkey

Correspondence author:
[*]Prof. Dr. Halise Inci Gul
Ataturk University,
Faculty of Pharmacy,
Department of Pharmaceutical Chemistry,
25240, Erzurum/TURKEY
Tel: +90 4422315219
Fax: +90 4422315201
E-mail: incigul1967@yahoo.com or incigul@atauni.edu.tr

Running Title: Bioactivities of pyrazoline-benzenesulfonamides

ABSTRACT

In the present study, 4-[5-aryl-3-(thiophen-2-yl)-4,5-dihydro-1*H*-pyrazol-1-yl] benzenesulfonamides were synthesized and inhibition effects on AChE, hCA I and hCA II were evaluated. K_i values of the compounds towards hCA I were in the range of 24.2±4.6-49.8±12.8 nM while they were in the range of 37.3±9.0-65.3±16.7 nM towards hCA II. K_i values of the Acetazolamide were 282.1±19.7 nM and 103.60±27.6 nM towards both isoenzymes, respectively. The compounds inhibited AChE with K_i in the range of 22.7±10.3-109.1±27.0 nM, whereas the Tacrine had Ki value of 66.5±13.8 nM. Electronic structure calculations at M06-L/6-31+G(d,p)//AM1 level and molecular docking studies were also performed to enlighten

This article has been accepted for publication and undergone full peer review but has not been through the copyediting, typesetting, pagination and proofreading process, which may lead to differences between this version and the Version of Record. Please cite this article as doi: 10.1111/cbdd.13149

inhibition mechanism and to support experimental findings. Results obtained from calculations of molecular properties showed that the compounds obey drug likeness properties. The experimental and computational findings obtained in the present study might be useful in the design of novel inhibitors against hCA I, hCA II, and AChE.

KEYWORDS: Carbonic anhydrase, acetylcholinesterase, pyrazoline, sulfonamide, docking, modeling

1. INTRODUCTION

Enzymes have attracted more interests as targets for drug discovery and development because of their important roles in many diseases. Among therapeutic agents in market today, almost half of them carry out their therapeutic effects by inhibiting or activating enzymes. Medicinal chemists are focused on the identification and optimization of drug candidates that act as enzyme inhibitors or activators.[1]

Carbon dioxide (CO_2) and bicarbonate (HCO_3^-) are essential compounds in living organisms[2]. Carbonic anhydrase (CAs, EC 4.2.1.1), a zinc-containing enzyme, catalyzes a reversible reaction between CO_2 hydration and HCO_3^- dehydration. CAs are present in many organisms and have an essential role in pathological and physiological events including pH regulation, bone resorption, carboxylation reactions, synthesis of bicarbonate, calcification, osteoporosis, glaucoma, cancer, and neurological disorders.[3-5] Sulfonamides, especially aromatic primary sulfonamides, have been reported as the most attractive scaffolds for the development of new CA inhibitors.[5] Sulfonamide derivatives such as acetazolamide, methazolamide, ethoxzolamide and celecoxib are used as CA inhibitors (CAIs) in many studies as reference drugs (Figure 1). [6,7]

Alzheimer's disease (AD) is a chronic progressive neurodegenerative disorder which is seen in people over 65 years old.[8] The number of people suffering from AD is increasing everyday and it is estimated that the number of patients will reach up to 100 million by the year 2050.[9] Annual cost of the treatment of AD patients is about $100 billion.[8] At present, there is no way to eradicate the AD. The drugs available on the market provide only palliative treatment and reduce the speed of disease.[10]

Cholinergic inhibition is one of the most essential way used for the patients with AD.[10] Acetylcholinesterase (AChE) is one of the most crucial enzymes for nerve response and function. It catalyzes the hydrolysis of acetylcholine to choline and acetic acide. AChE is widely distributed in a variety of nerve muscle tissue in the brain.[8] Tacrine, donepezil, rivastigmine and galantamine are amongst the drugs that are currently being used in clinics as acetylcholinesterase inhibitors (Figure 1).[10]

Pyrazolines, as one of the most important heterocyclic compounds in medicinal chemistry, have various biological activities such as anti-Alzheimer[11,12], anti-Parkinson[13] and antidepressant.[14,15] They show their effects by inhibiting or activating several enzymes such as cholinesterases, monoamine oxidases and carbonic anhydrases. Ucar et al. have reported several N-substituted pyrazoline derivatives as monoamine oxidases-B and cholinesterase inhibitors with the promising activity, which can be useful for the development of new drug candidates for Alzheimer and Parkinson diseases.[13] In addition, the compounds having sulfonamide core were also found as promising compounds, which can be considered to develop new potent AChE inhibitors since they presented valuable results in AChE inhibition tests. [16,17] Besides, sulfonamides are known with several bioactivities such as diuretic, antigloucoma, anticonvulsant, and antiobesity. [18,19,20]

Pharmacophore hybrid approach is one of the most effective method in medicinal chemistry to produce new drug candidates.[21] It includes the combination of two or more pharmacophore groups in a single molecule to obtain synergetic effect. It also provides a modified selectivity profile with improved pharmacokinetic and pharmacodynamic restrictions, reduction of undesirable side effects, having dual or multiple modes of action, and less drug-drug interactions.[21] This method has been successfully used by several researchers and has had very remarkable results with diseases having multifactorial profiles such as Alzheimer´s disease, Parkinson´s disease, cancer, inflammation, and hypertension.[21]

In the present study, it was aimed to synthesize compounds **TP1-10**, 4-[5-aryl-3-(thiophen-2-yl)-4,5-dihydro-1*H*-pyrazol-1-yl] benzenesulfonamides, bearing sulfonamide and pyrazoline moieties, which are known to have CA and/or AChE inhibitory properties in a single molecule. Aryl part was changed in the design as nonsubstituted/substituted phenyl or thiophen-2-yl to see the effects of different aromatic rings and substituents having different electronic nature on AChE, hCA I and hCA II enzymes. In addition, molecular modeling

studies were also considered as a value added tool in understanding the inhibition mechanism at molecular level and to enlighten the interactions of the synthesized compounds with their corresponding target.

2. METHODS AND MATERIALS

2.1 Chemistry

The chemical structures of the compounds **TP1-10** were confirmed by the Nuclear Magnetic Resonance (NMR) spectra ^{1}H NMR (400 MHz) and ^{13}C NMR (100 MHz) (Varian Mercury Plus spectrometer, Varian inc., Palo Alto, California, U.S.). Chemical shifts (δ) are reported in ppm and coupling constants (*J*) are expressed in hertz (Hz). Mass spectra (HRMS) for the compounds were taken using a liquid chromatography ion trap-time of flight tandem mass spectrometer (Shimadzu, Kyoto, Japan) equipped with an electrospray ionization (ESI) source, operating in both positive and negative ionization modes. Shimadzu's LCMS Solution software was used for data analysis. Melting points were determined using an Electrothermal 9100/IA9100 instrument (Bibby Scientific Limited, Staffordshire, UK) and are uncorrected.

2.2 General synthesis method of the pyrazolines TP 1-10, Scheme 1

First, chalcones were synthesized via Claisen-Schmidt reaction as described in literatures. [22-28] 2-Acetylthiophene (2 g, 16 mmol) and the appropriate aromatic aldehyde (1.7 g for **1**, 2.0 g for **2**, 2.2 g for **3**, 2.0 g for **4**, 2.2 g for **5**, 3.0 g for **6**, 2.8 g for **7**, 1.8 g for **8**, 2.6 g for **9**, 2.6 g for **10,** 16 mmol) were dissolved in ethanol (10 mL) and an aqueous solution of potassium hydroxide (10 mL, 40% w/v) was added dropwise into the reaction flask. Reaction mixtures were stirred for 3-6 hours at room temperature and reactions were followed by thin layer chromatography (TLC) using dichloromethane:methanol (4.8:0.2) solvent system. After completion of the reaction, the reaction mixture was poured into the water (25 mL) and then acidified with hydrochloric acid solution (10%) to pH=3-4. The solid obtained was filtered, washed with water and ethanol for several times. The purity of the chalcones (Compounds **1-10**, Scheme 1) was checked by TLC and then they were used in the synthesis of pyrazolines (Compounds **1-10**, Scheme 1) without further purification.

At the second step, a solution of the appropriate chalcone (0.5 g, 2 mmol) in ethanol (30 mL) with glacial acetic acid (0.1 ml) was heated until chalcone dissolved and then *p*-hydrazinobenzene sulfonamide hydrochloride (0.5 g, 2 mmol) was added into the reaction mixture and finally, the mixture was refluxed for 22 h. [22-26] The reactions were monitored by

TLC plates using chloroform:methanol (5 mL:2 drops) as solvent system. After completion of the reaction, the mixture was poured into the water (50 mL). The solid compounds obtained were filtered and dried. The compounds **TP1** (ethanol), **TP3** (methanol/chloroform), **TP4** (methanol/chloroform), **TP7** (ethanol/dichloromethane), **TP8** (ethanol/chloroform), **TP9** (ethanol/acetone) were purified by crystallization from suitable solvent. On the other hand, the compounds **TP2**, **TP5**, **TP6**, and **TP10** were first purified by using column chromatography (with chloroform) and then crystallization (dichloromethane/diisopropyl ether), respectively. The chemical structures of the pyrazolines were confirmed using ^{1}H NMR (400 MHz) and ^{13}C NMR (100 MHz) and HRMS spectra. Physical and spectral data for the compounds **TP 1-10** are listed below.

2.2.1 4-(5-Phenyl-3-(thiophen-2-yl)-4,5-dihydro-1H-pyrazol-1-yl)benzenesulfonamide (TP1)[29]

Light yellow solid. Mp 212-214 °C. Yield 11%. ^{1}H NMR (400 MHz, DMSO-*d6*, δ_{ppm}) 7.65 (dd, *J*=5.1, 1.1 Hz, 1H, ArH), 7.55 (d, *J*= 9.1 Hz, 2H, ArH), 7.35-7.31 (m, 3H, ArH), 7.26-7.22 (m, 3H, ArH), 7.10 (dd, *J*=4.8, 3.7 Hz, 1H, ArH), 7.00 (s, 2H, -SO_2NH_2), 6.97 (d, *J*=8.8 Hz, 2H, ArH), 5.62 (dd, *J*= 12.0, 5.0 Hz, 1H, pyrazoline ring), 3.96 (dd, *J*=17.4, 12.0 Hz, 1H, pyrazoline ring), 3.17 (dd, *J*=17.4, 5.0 Hz, 1H, pyrazoline ring). ^{13}C NMR (100 MHz, DMSO-*d6*, δ_{ppm}) 146.6, 146.3, 142.1, 135.7, 133.7, 129.8, 129.3, 129.0, 128.7, 128.4, 127.9, 126.4, 112.6, 63.0, 44.4. HRMS (ESI-MS) *m/z* Calculated for $C_{19}H_{16}N_3O_2S_2$ $[M-H]^-$ 382.0577; found 382.0590.

2.2.2 4-(3-(Thiophen-2-yl)-5-(p-tolyl)-4,5-dihydro-1H-pyrazol-1-yl)benzenesulfonamide (TP2)

Beige solid. Mp 198-199 °C. Yield 14 %. ^{1}H NMR (400 MHz, DMSO-*d6*, δ_{ppm}) 7.64 (d, *J*=4.8 Hz, 1H, ArH), 7.54 (d, *J*= 8.8 Hz, 2H, ArH), 7.30 (d, *J*=3.3 Hz, 1H, ArH), 7.14-7.01 (m, 5H, ArH), 6.97 (d, *J*=9.1 Hz, 2H, ArH), 6.99 (s, 2H, -SO_2NH_2), 5.57 (dd, *J*= 12.0, 5.0 Hz, 1H, pyrazoline ring), 3.94 (dd, *J*=17.5, 12.0 Hz, 1H, pyrazoline ring), 3.14 (dd, *J*=17.5, 5.0 Hz, 1H, pyrazoline ring), 2.48 (s, 3H, -CH_3). ^{13}C NMR (100 MHz, DMSO-*d6*, δ_{ppm}) 146.6, 146.3, 139.1, 137.6, 135.7, 133.6, 130.3, 129.2, 128.9, 128.6, 127.8, 126.3, 112.6, 62.8, 44.4, 21.3. HRMS (ESI-MS) *m/z* Calculated for $C_{20}H_{18}N_3O_2S_2$ $[M-H]^-$ 396.0734; found 396.0733.

2.2.3 4-(5-(4-Methoxyphenyl)-3-(thiophen-2-yl)-4,5-dihydro-1H-pyrazol-1-yl) benzenesulfonamide (TP3) [29,30]

Light yellow solid. Mp 188-190 °C, 160-162°C[30]. Yield 22 %. ^{1}H NMR (400 MHz, DMSO-*d6*, δ_{ppm}) 7.63 (dd, *J*=4.9, 1.1 Hz, 1H, ArH), 7.55 (d, *J*= 9.1 Hz, 2H, ArH), 7.30 (dd, *J*= 3.7, 1.1 Hz, 1H, ArH), 7.14 (d, *J*= 8.8 Hz, 2H, ArH), 7.10 (dd, *J*=4.9, 3.7 Hz, 1H, ArH), 7.00 (s, 2H, -SO_2NH_2), 6.98 (d, *J*=8.8 Hz, 2H, ArH), 6.87 (d, *J*=8.4 Hz, 2H, ArH), 5.56 (dd, *J*= 12.0, 5.0 Hz, 1H, pyrazoline ring), 3.92 (dd, *J*=17.5, 12.0 Hz, 1H, pyrazoline ring), 3.68 (s, 3H, -OCH_3), 3.15 (dd, *J*=17.5, 5.0 Hz, 1H, pyrazoline ring). ^{13}C NMR (100 MHz, DMSO-*d6*, δ_{ppm}) 159.3, 146.6, 146.3, 135.8, 133.9, 133.6, 129.3, 128.9, 128.6, 127.8, 127.6, 115.2, 112.6, 62.6, 55.8, 44.5. HRMS (ESI-MS) *m/z* Calculated for $C_{20}H_{18}N_3O_3S_2$ $[M-H]^-$ 412.0683; found 412.0689.

2.2.4 4-(5-(4-Fluorophenyl)-3-(thiophen-2-yl)-4,5-dihydro-1H-pyrazol-1-yl) benzenesulfonamide (TP4)

Light yellow solid. Mp 209-210 °C. Yield 30 %. ^{1}H NMR (400 MHz, DMSO-*d6*, δ_{ppm}) 7.65 (d, *J*=5.3 Hz, 1H, ArH), 7.57 (d, *J*=8.8 Hz, 2H, ArH), 7.32 (dd, *J*=3.3 Hz, 1H, ArH), 7.27 (dd, *J*= 8.8, 5.3 Hz, 2H, ArH), 7.16 (t, *J*=8.8 Hz, 2H, ArH), 7.10 (dd, *J*= 4.8, 3.7 Hz, 1H, ArH), 7.02 (s, 2H, -SO_2NH_2), 6.96 (d, *J*=8.8 Hz, 2H, ArH), 5.65 (dd, *J*= 12.0, 5.0 Hz, 1H, pyrazoline ring), 3.95 (dd, *J*=17.6, 12.0 Hz, 1H, pyrazoline ring), 3.17 (dd, *J*=17.6, 5.0 Hz, 1H, pyrazoline ring). ^{13}C NMR (100 MHz, DMSO-*d6*, δ_{ppm}) 162.1 ($^{1}J_{CF}$=243.4 Hz), 146.6, 146.1, 138.2 ($^{4}J_{CF}$=2.6 Hz), 135.6, 133.8, 129.4, 129.2, 129.1 ($^{3}J_{CF}$=7.6 Hz), 128.6, 127.9, 116.7 ($^{2}J_{CF}$=21.4 Hz), 112.6, 62.3, 44.3. HRMS (ESI-MS) *m/z* Calculated for $C_{19}H_{17}N_3O_2FS_2$ $[M+H]^+$ 402.0741; found 402.0740.

2.2.5 4-(5-(4-Chlorophenyl)-3-(thiophen-2-yl)-4,5-dihydro-1H-pyrazol-1-yl) benzenesulfonamide (TP5)[30]

Beige solid. Mp 189-191 °C, 136-138°C[30]. Yield 10 %. ^{1}H NMR (400 MHz, DMSO-*d6*, δ_{ppm}) 7.65 (dd, *J*=5.0, 1.1 Hz, 1H, ArH), 7.57 (d, *J*=8.8 Hz, 2H, ArH), 7.39 (d, *J*=8.6 Hz, 2H, ArH), 7.31 (dd, *J*= 3.7, 1.1 Hz, 1H, ArH), 7.24 (d, *J*=8.6 Hz, 2H, ArH), 7.10 (dd, *J*= 5.0, 3.7 Hz, 1H, ArH), 7.02 (s, 2H, -SO_2NH_2), 6.97 (d, *J*=8.8 Hz, 2H, ArH), 5.66 (dd, *J*= 12.0, 5.0 Hz, 1H, pyrazoline ring), 3.96 (dd, *J*=17.5, 12.0 Hz, 1H, pyrazoline ring), 3.19 (dd, *J*=17.6, 5.0 Hz, 1H, pyrazoline ring). ^{13}C NMR (100 MHz, DMSO-*d6*, δ_{ppm}) 146.7, 146.1, 140.9, 135.5, 133.9, 132.9, 129.8, 129.5, 129.1, 128.6, 128.4, 127.9, 112.6, 62.3, 44.1. HRMS (ESI-MS) *m/z* Calculated for $C_{19}H_{17}N_3O_2S_2Cl$ $[M+H]^+$ 418.0445; found 418.0445.

2.2.6 4-(5-(4-Bromophenyl)-3-(thiophen-2-yl)-4,5-dihydro-1H-pyrazol-1-yl) benzenesulfonamide (TP6)

Light green solid. Mp 215-217 °C. Yield 16 %. ^{1}H NMR (400 MHz, DMSO-*d6*, δ_{ppm}) 7.65 (dd, *J*=5.0, 1.1 Hz, 1H, ArH), 7.57 (d, *J*=8.9 Hz, 2H, ArH), 7.53 (d, *J*=8.6 Hz, 2H, ArH), 7.31 (dd, *J*= 3.5, 1.1 Hz, 1H, ArH), 7.18 (d, *J*=8.6 Hz, 2H, ArH), 7.10 (dd, *J*= 5.0, 3.5 Hz, 1H, ArH), 7.02 (s, 2H, -SO_2NH_2), 6.97 (d, *J*=8.9 Hz, 2H, ArH), 5.64 (dd, *J*= 12.0, 5.0 Hz, 1H, pyrazoline ring), 3.95 (dd, *J*=17.5, 12.0 Hz, 1H, pyrazoline ring), 3.18 (dd, *J*=17.5, 5.0 Hz, 1H, pyrazoline ring). ^{13}C NMR (100 MHz, DMSO-*d6*, δ_{ppm}) 146.7, 146.1, 141.4, 135.5, 133.9, 132.8, 129.4, 129.3, 129.1, 128.7, 127.9, 121.4, 112.7, 62.4, 44.2. HRMS (ESI-MS) *m/z* Calculated for $C_{19}H_{17}N_3O_2S_2Br$ $[M+H]^+$ 461.9940; found 461.9939.

2.2.7 4-(3-(Thiophen-2-yl)-5-(4-(trifluoromethyl)phenyl)-4,5-dihydro-1H-pyrazol-1-yl) benzenesulfonamide (TP7) [30]

Beige solid. Mp 198-200 °C, 260-262 °C[30]. Yield 40 %. ^{1}H NMR (400 MHz, DMSO-*d6*, δ_{ppm}) 7.72 (d, *J*=8.1 Hz, 2H, ArH), 7.65 (d, *J*=5.1 Hz, 1H, ArH), 7.57 (d, *J*=8.8 Hz, 2H, ArH), 7.44 (d, *J*= 8.1 Hz, 2H, ArH), 7.31 (d, *J*=3.7 Hz, 1H, ArH), 7.11-7.09 (m, 1H, ArH), 7.02 (s, 2H, -SO_2NH_2), 6.98 (d, *J*=8.8 Hz, 2H, ArH), 5.76 (dd, *J*= 12.1, 4.8 Hz, 1H, pyrazoline ring), 4.00 (dd, *J*=17.6, 12.1 Hz, 1H, pyrazoline ring), 3.23 (dd, *J*=17.6, 4.8 Hz, 1H, pyrazoline ring). ^{13}C NMR (100 MHz, DMSO-*d6*, δ_{ppm}) 146.7, 146.1, 135.4, 133.9, 129.6, 129.4, 129.3, 129.2, 128.3, 127.3, 126.8, 112.7, 112.5, 62.5, 44.1. HRMS (ESI-MS) *m/z* Calculated for $C_{20}H_{17}F_3N_3O_2S_2$ $[M+H]^+$ 452.0709; found 452.0708.

2.2.8 4-(3,5-Di(thiophen-2-yl)-4,5-dihydro-1H-pyrazol-1-yl benzenesulfonamide (TP8) [30]

Light brown solid. Mp 226-227 °C, 218-220°C[30]. Yield 22 %. ^{1}H NMR (400 MHz, DMSO-*d6*, δ_{ppm}) 7.67 (dd, *J*=5.0, 1.1 Hz, 1H, ArH), 7.59 (d, *J*=9.1 Hz, 2H, ArH), 7.38-7.36 (m, 2H, ArH), 7.13 (dd, *J*=3.7, 1.2 Hz, 2H, ArH), 7.10 (d, *J*= 9.1 Hz, 2H, ArH), 7.04 (s, 2H, -SO_2NH_2), 6.93 (dd, *J*=5.2, 3.4 Hz, 1H, ArH), 5.99 (dd, *J*= 11.5, 4.5 Hz, 1H, pyrazoline ring), 3.92 (dd, *J*=17.4, 11.5 Hz, 1H, pyrazoline ring), one of the signal of protons on pyrazoline ring was observed under solvent peak. ^{13}C NMR (100 MHz, DMSO-*d6*, δ_{ppm}) 147.0, 146.4, 144.9, 135.6, 134.2, 129.4, 129.2, 128.7, 127.8, 127.7, 127.5, 126.3, 113.1, 59.2, 44.4. HRMS (ESI-MS) *m/z* Calculated for $C_{17}H_{14}N_3O_2S_3$ $[M+H]^+$ 390.0399; found 390.0403

2.2.9 4-(5-(2,4-Dimethoxyphenyl)-3-(thiophen-2-yl)-4,5-dihydro-1H-pyrazol-1-yl) benzenesulfonamide (TP9)

Light green solid. Mp 205-206 °C. Yield 35 %. ^{1}H NMR (400 MHz, DMSO-*d6*, δ_{ppm}) 7.62 (dd, *J*=5.1, 1.1 Hz, 1H, ArH), 7.56 (d, *J*=9.1 Hz, 2H, ArH), 7.30 (dd, *J*=3.7, 1.1 Hz, 1H, ArH), 7.09 (dd, *J*= 5.1, 3.7 Hz, 1H, ArH), 7.00 (s, 2H, -SO_2NH_2), 6.90 (d, *J*=8.8 Hz, 2H, ArH), 6.73 (d, *J*=8.4 Hz, 1H, ArH), 6.62 (dd, *J*= 2.3 Hz, 1H, ArH), 6.39 (dd, *J*=8.4, 2.3 Hz, 1H, ArH), 5.62 (dd, *J*=12.0, 5.0 Hz, 1H, pyrazoline ring), 3.89 (dd, *J*=17.6, 12.0 Hz, 1H, pyrazoline ring), 3.86 (s, 3H, -OCH_3), 3.69 (s, 3H, -OCH_3), 3.05 (dd, *J*=17.6, 5.0 Hz, 1H, pyrazoline ring). ^{13}C NMR (100 MHz, DMSO-*d6*, δ_{ppm}) 160.8, 157.8, 147.1, 146.2, 135.9, 133.4, 129.1, 129.0, 128.8, 127.9, 120.8, 112.3, 112.2, 105.6, 99.7, 57.8, 56.5, 55.9, 43.3. HRMS (ESI-MS) *m/z* Calculated for $C_{21}H_{22}N_3O_4S_2$ $[M+H]^+$ 444.1046; found 444.1042.

2.2.10 4-(5-(3,4-Dimethoxyphenyl)-3-(thiophen-2-yl)-4,5-dihydro-1H-pyrazol-1-yl) benzenesulfonamide (TP10)

Beige solid. Mp 168-170 °C. Yield 12 %. ^{1}H NMR (400 MHz, DMSO-*d6*, δ_{ppm}) 7.63 (dd, *J*=5.1, 1.1 Hz, 1H, ArH), 7.55 (d, *J*=8.8 Hz, 2H, ArH), 7.30 (dd, *J*=3.7, 1.1 Hz, 1H, ArH), 7.09 (dd, *J*= 5.1, 3.7 Hz, 1H, ArH), 7.01 (s, 1H, ArH), 6.99 (d, *J*=8.8 Hz, 2H, ArH), 6.91 (s, 2H, -SO_2NH_2), 6.85 (d, *J*=8.4 Hz, 1H, ArH), 6.63 (dd, *J*=8.4, 2.2 Hz, 1H, ArH), 5.51 (dd, *J*=12.0, 5.1 Hz, 1H, pyrazoline ring), 3.89 (dd, *J*=16.9, 12.0 Hz, 1H, pyrazoline ring), 3.69 (s, 3H, -OCH_3), 3.66 (s, 3H, -OCH_3), 3.16 (dd, *J*=16.9, 5.1 Hz, 1H, pyrazoline ring). ^{13}C NMR (100 MHz, DMSO-*d6*, δ_{ppm}) 149.7, 148.8, 146.7, 146.5, 135.7, 134.3, 133.6, 129.2, 128.9, 128.7, 127.8, 118.0, 112.8, 112.7, 110.3, 63.0, 56.1, 56.0, 44.5. HRMS (ESI-MS) *m/z* Calculated for $C_{21}H_{22}N_3O_4S_2$ $[M+H]^+$ 444.1046; found 444.1043.

2.3 Biological activity

2.3.1 Purification and inhibition studies of carbonic anhydrase (CA) I and II isoforms

In the current study, CA isoforms (hCA I and II) using sepharose-4B-Lyrosine-sulfanilamide affinity chromatography were purified in a single purification stage using fresh human blood erythrocytes and the erythrocytes samples were centrifuged at 13000 rpm for 30 min and the buffy buffy coat and plasma were discarded. Also, pH of the buffer was slowly adjusted to 8.7, by using solid Tris.[22-25] Additionally, after centrifugation, supernatant was transferred to the Sepharose-4B-L-Tyrosine-sulphanilamide affinity column that was previously prepared.[31] The enzymes from the column were then spectrophotometrically measured at 280 nm. Sodium dodecyl sulphate–polyacrylamide gel electrophoresis (SDS–PAGE) was

examined for registration of both isoforms purity.[32] Human CA isoforms activity designation was observed spectrophotometrically (Shimadzu, UV-VIS Spectrophotometer, UVmini-1240, Kyoto, Japan).[33] In this test, variations in absorbance were obtained during 3 min at 30 ºC. *p*-Nitrophenylacetate (NPA) molecule was used as substrate and transformed by both isoforms to *p*-nitrophenolate ion.[32] For description of protein quantity at the purification stages, Bradford process was used.[34] The bovine serum albumin molecule was used as control factor for this definition, which was done at 595 nm. For obtaining the inhibition results of each isoform, the compounds **TP1-10** and an activity (%) [**TP1-10**] graph was drawn. To calculate K_i values, three diverse [**TP1-10**] concentrations were studied. Acetazolamide (AZA) was used as a reference compound.

2.3.2 Determination of Acetylcholinesterase (AChE) activity

The inhibitory efficacy of the compounds **TP1-10** on AChE activity was tested following the spectrophotometric process of Ellman test.[35] Acetylthiocholine iodide (AChI) was used as substrates.[36,37] For the mensuration of the AChE activity, 5,5'-dithio-bis(2-nitro-benzoic)acid compound (DTNB, D8130-1G, Sigma-Aldrich, Steinheim, Germany) was applied.[38] Briefly, 50 µL DTNB and 100 µL of Tris/HCl solution (1M, pH 8.0), 750 mL of sample solution dissolved in distilled water at disparate concentrations and 50 µL AChE (5.32×10^{-3} U) solution were incubated and mixed for 15 min at 30 ºC. Finally, the reaction was started by adding 50 µL of AChI. The enzymatic hydrolysis of this substrate which produces a yellow 5-thio-2-nitrobenzoate anion as the result of the product of thiocholine with DTNB, was recorded spectrophotometrically at a wavelength of 412 nm.[37] Tacrine (TAC) was used as a reference compound.

2.4 Computational section

2.4.1 Molecular docking

The ligand preparation and protein preparation steps are necessary to ensure that the structures meet minimum requirements for further computational calculations. LigPrep tool (Schrödinger Release 2016-4: LigPrep, Schrödinger, LLC, New York, NY, 2016) interfaced with Maestro module of Schrödinger suite was used for the preparation of all the molecules including the reference compounds, Tacrine and Acetazolamide. All possible tautomer and ionization states at pH 7.0 ± 2.0 were generated. The compounds were then minimized using optimized potential liquid simulations 3 (OPLS3) force field.[39]

High-resolution protein crystal structures of acetylcholinesterase (AChE), carbonic anhydrase (CA) I, and II (PDB Ids: 1DX6, 2NMX and 3HS4, respectively) were downloaded from RCSB Protein Data Bank and used for molecular docking. All X-ray crystal structures were in complexed with a native ligand. As a first step, protein Preparation Wizard (PrepWizard, Schrödinger Release 2016-4: Schrödinger Suite 2016-4 Protein Preparation Wizard; Epik, Schrödinger, LLC, New York, NY, 2016; Impact, Schrödinger, LLC, New York, NY, 2016; Prime, Schrödinger, LLC, New York, NY, 2016)[40] in Maestro of Schrödinger software package (Schrödinger Release 2016-4, Maestro. Schrödinger, LLC, New York, NY, 2016) were used to prepare crystal structures. Bond orders were assigned and hydrogens were added to the structures. The native ligands in all structures were kept for defining the binding sites and in case of carbonic anhydrases; zinc metal was also retained being a key moiety in the active site. All water molecules and heteroatoms were then removed. The final structures were optimized and finally minimized using OPLS3 force field. This helps to avoid steric clashes between the atoms.

A grid that represents the binding pocket was generated using the co-crystallized native ligands as reference. Default settings were applied in each case. Glide SP (standard precision) module of Schrödinger Suite[41,42] was used to dock the synthesized compounds into the active site of the crystal structures.

2.4.2 Calculation of physicochemical and ADME properties

QikProp module of Schrodinger (Schrödinger Release 2016-4, QikProp. Schrödinger, LLC, New York, NY, 2016) was used to calculate some molecular descriptors commonly used in absorption, distribution, metabolism and excretion (ADME) analysis. Frontier molecular orbital (HOMO and LUMO) energy values and dipole moments were calculated using Wave function's Spartan'16 parallel suite (Spartan 16, Wavefunction Inc., Irvine CA). As a first step, the geometry of all compounds was optimized at AM1 level. Frequency calculations were also calculated to verify that this optimized geometry is a real minimum on the potential energy surface with no imaginary frequencies. Single point energy calculation was computed at M06-L level using the popular polarized basis set, 6-31+G(d,p), which adds p functions to hydrogen atoms and d functions on heavy atoms.

3. RESULTS

3.1 Chemistry

The compounds **TP1-10**, 4-[5-aryl-3-(thiophen-2-yl)-4,5-dihydro-1*H*-pyrazol-1-yl] benzenesulfonamides, were synthesized successfully. Aryl part was changed as phenyl (**TP1**), 4-methylphenyl (**TP2**), 4-methoxyphenyl (**TP3**), 4-fluorophenyl (**TP4**), 4-chlorophenyl (**TP5**), 4-bromophenyl (**TP6**), 4-trifluoromethylphenyl (**TP7**), thiophen-2-yl (**TP8**), 2,4-dimethoxyphenyl (**TP9**) and 3,4-dimethoxyphenyl (**TP10**). The compounds **TP2**, **TP4**, **TP6**, **TP9** and **TP10** were reported for the first time in this study. The compounds **TP1**, **TP3**, **TP5**, **TP7** and **TP8** were registered in literatures as racemates and their several bioactivities such as antidiabetic, anticancer, anti-inflammatory and COX inhibitory activities were reported.[29,30] The compounds synthesized in this study were also obtained as pure racemates and they were directly used for CA and AChE inhibiton studies.

Structures of the compounds synthesized were established on the basis of spectral data taken from ^{1}H NMR, ^{13}C NMR and HRMS. In the ^{1}H NMR and ^{13}C NMR spectra of the compounds **TP1-10**, chemical shift values of the three hydrogen atoms attached to the C-4 and C-5 carbon atoms of the pyrazoline ring and C-4 and C-5 carbon atoms of the pyrazolines were observed as expected. [25,26] The appearance of three doublets in the range of δ 5.99-3.05 ppm confirmed the formation of pyrazole ring, except **TP8** (one of the signals of proton on pyrazole ring was hidden under DMSO peak). Two carbon atoms of pyrazoline ring (C-4 and C-5) were appeared around 63.0 ppm and 44.0 ppm. The signal of protons on SO_2NH_2 group were observed in the range of δ 7.04-6.99 pm as a singlet. Mass spectra showing $[M+H]^+$ or $[M-H]^-$ peaks further confirmed the synthesis of desired compounds.

3.2 Bioactivity Studies

The inhibition of human CA isoforms I, and II with the compound **TP1-10** was reported for the first time and the inhibition data are shown in Table 1. The inhibitory effects of the compounds **TP1-10** on AChE enzyme are also reported for the first time and the inhibition data are shown in Table 1. Selectivity ratios of the compounds on enzymes are calculated and data are presented in Table 3.

3.2.1 Carbonic anhydrase inhibitory effects

The compounds having sulfonamide pharmacophore have been reported with high binding affinities for most of CA isoenzymes.[18] In this study, the compounds were designed to have sulfonamide moiety as one of the pharmacophores. The compounds **TP1-10** have shown better inhibitory activities than the reference drug Acetazolamide (AZA). According to Table 1, K_i values of the compounds towards hCA I were in the range of 24.2±4.6 - 49.8±12.8 nM, while they were in the range of 37.3±9.0 - 65.3±16.7 nM towards hCA II isoenzyme. K_i values of acetazolamide (AZA) were 282.1±19.7 nM and 103.6±27.6 nM towards both isoenzymes, respectively. When K_i values were considered it was difficult to decide about the lead compound towards hCA I, and II, since K_i values were similar, although they were lower than K_i values of AZA. It was also noticed that K_i values of the compounds towards hCA I were less than the K_i values towards hCA II.

3.2.2 Acetylcholinesterase inhibitory effects

Most of the compounds effectively inhibited AChE at nanomolar level. When K_i values of the compounds considered towards AChE, they were in the range of 22.7±10.3 -109.1±27.0 nM while the reference drug Tacrine (TAC) had K_i value as 66.5±13.8 nM. K_i values of the compounds pointed out the compound **TP2** with the lowest value, as the most potent compound while **TP10** was the least effective one towards AChE.

3.2.3 Selectivity of the compounds on enzymes

Selectivity Ratio (SR) value reflects the selectivity of a compound towards hCA I or II isoenzymes. The SR values were calculated by dividing Ki value of the certain compounds to hCA II or hCA I. Potency Selectivity Ratios (PSR1 and PSR2) of a compound towards hCA I and II were also calculated. PSR1 values were produced by dividing Ki value of AZA (282.090 nM) to Ki value of a certain compound towards hCA I. PSR2 values were produced by dividing Ki value of AZA (103.60 nM) to Ki value of a certain compound towards hCA II. In addition, PSR3 values of the compound towards AChE were also calculated. Reference compound was TAC. PSR3 values were produced by dividing Ki value of TAC (66.521 nM) to Ki value of a certain compound towards AChE. Data were presented in Table 3.

Based on the Table 3, SR values of the compounds calculated were between 0.9-1.9. According to these values, the compounds were found to be 2.3-4.8 fold more selective than

reference drug AZA towards hCA I isoenyzme but their selectivity towards hCA II were not higher than AZA.

PSR1 values of the compounds were in the range of 5.7-11.7. The compound **TP8** (PSR1=11.7) bearing thiophene is the most selective one towards hCA I. Additionally, having the SR values between 1.7-2.8, the compounds were found to be more selective towards hCA II than AZA. The compound **TP6** (PSR1=2.8) bearing 4-bromophenyl was the most selective one towards hCA II. According to PSR1 and PSR2 values, it can be said that compounds were found to be more selective towards hCA I than hCA II isoenzyme.

On the other hand, except **TP3**, **TP6**, **TP10**, other compounds were effectively inhibited AChE enzyme. Seven of the compounds had selectivity ratios higher than 1. The compounds **TP2** (PSR3=2.9) bearing 4-mehylphenyl and **TP7** (PSR3=2.3) bearing 4-trifluoromethylphenyl can be considered as lead inhibitor compounds of this study towards AChE enzyme to design new AChE inhibitors.

3.3 Computational Section

As a first step, we have calculated some molecular descriptors commonly used in absorption, distribution, metabolism and excretion (ADME) analysis (Table 2). Accordingly, molecular weight (MW), predicted octanol/water partition coefficient (QplogPo/w), percent human oral absorption, polar surface area (PSA) and number of violations of Lipinski's rule of five of the incorporated ligands were estimated using QikProp module of Maestro molecular modeling package. All compounds obeys Lipinski's rule of five[43] which is an indication of the drug-likeness of a molecule, and PSA values are within the range that Veber *et. al.* suggested.[44]

Furthermore, several studies report the importance of dipole moment and the energy of frontier molecular orbitals having important contributions to the AChE inhibitory activity.[45,46] Hence, we found it necessary to calculate the quantum chemical properties of **TP1-10** and of **TAC** for comparison, at a high and accurate level (M06-L/6-31+G(d,p)//AM1).[47] The results agree well with the experimental findings. All active compounds have high dipole moments and high HOMO energy values in Table 2. The most active compound **TP7** has the highest dipole moment and its HOMO energy value is higher than the reference molecule **TAC** itself. In fact, HOMO energy values of all the compounds are higher than **TAC**.

In an attempt to get insight into the interaction of the synthesized compounds with the target receptors, molecular docking simulations were also carried out. Thus, all compounds were docked into the active sites of the AChE, CA I, and II separately. Docking scores in terms of binding energies were calculated and are given in Table 2. Despite the fact that the present docking algorithms fail to discriminate between active and inactive compounds in a high success rate[48,49], glide docking performed well in ranking the most active compounds especially for AChE and CAII.

2D ligand interaction diagrams are shown in Figure 2 (a-c). As can be seen from Figure 2a, the *R* configuration of the most active compound **TP7** makes key interactions with the binding pocket of AChE. However, the *S*-enantiomer failed to generate any poses. Hence, we believe that the active form is most probably **(*R*)-TP7**. The aromatic sulfonamide moiety of **TP7** orient itself deeply into the active site region establishing a hydrogen bond with the glutamic residue, GLH199, located at the anionic subsite. It also makes π-π contacts with HIS440 (one of the components of the estaric site) and Phe330 (the aromatic residue situated at the midpoint of the gorge).

On the other hand, the compounds showed high activities against CAI and CAII and their IC_{50} ranges were very close to each other. As can be seen from Table 2, with the exception of only **TP4**, the compounds scored higher than the reference compound, **AZA** against CAI. Sulfonamide groups in the most active compound **TP8**, adopts similar orientation with **AZA**, making the key interactions with the Thr199 and zinc ion in the catalytic binding site (Figure 2b). Same key interactions exist in the **TP1-CAII** complex, too (Figure 2c). Besides interaction with THR199 and zinc ion, the oxygen of the sulfonamide moiety forms an extra hydrogen bond with backbone amine group of Thr200.

4. DISCUSSION

The aim of a bioisosteric replacement is to design a new molecule with similar biological properties to the parent compound. The replacement can reduce toxicity, optimize activity of the lead molecule, and/or alter pharmacokinetics or the toxicity of the lead molecule. [50] In present study, 5^{th} position of pyrazoline ring was substituted with phenyl or substituted phenyl ring having different electronic nature or thiophene ring which is a bioisoster of phenyl ring. Several bioactivity data related to inhibitory effects of the compounds on hCA I, hCA II and AChE were obtained which lead to produce SAR data.

The cytosolic isoform hCA I was inhibited by all compounds investigated here in nanomolar range, with IC_{50} in the range of 25.7-45.8 nM. All compounds were found 6.5-11.6 times more potent than the reference drug AZA (IC_{50}=297.1 nM) according to IC_{50} values. When *para* position of phenyl ring was substituted with methyl group, inhibition potency of the compound **TP2 (**IC_{50}=30.1 nM) increased slightly (1.1 times) compared with **TP1** (IC_{50}=34.7 nM) which has non-substituted phenyl. When the methyl group was replaced with methoxy group (**TP3,** IC_{50}=36.5 nM) the inhibitory activity of the compound slightly decreased comparing **TP1**. On the other hand, introduction of dimethoxy groups (**TP9**, IC_{50}=45.8 nM; **TP10**, IC_{50}=40.5 nM) on phenyl decreased the inhibitory activity of the compounds towards hCA I compared with **TP1**'s**.**

When hydrogen at *para* position of phenyl ring was replaced by a halogen, inhibition effect increased only in the compound **TP6** having bromine substituent (IC_{50}=27.7 nM) compared with **TP1** (IC_{50}=34.7 nM). The general trend for hCA I inhibition potency of the compounds was in the order of Br (IC_{50}=27.7 nM) > Cl (IC_{50}=34.5 nM) > F (IC_{50}=40.8 nM), which is inversely correlated by electronegativity of the substituents. It can be said that electronegativity and size of halogen affected the inhibition capability of the compounds. Bioisosteric replacement of the phenyl by thiophen ring was found to be a useful modification in present study to increase the inhibitory effects on hCA I. According to IC_{50} values, the compound **TP8** (IC_{50}= 25.7 nM) having the thiopene ring was the most effective one. It was 11.6 fold more potent inhibitor than AZA (IC_{50}=297.1nM). In addition, **TP8** was the best inhibitor towards hCA I isoenzyme among others according to IC_{50} value.

The isoform hCA II was inhibited by the compounds reported in this study at nanomolar concentration with IC_{50} in the range of 33.0-57.8 nM. All compounds were found 2.0-3.5 more potent than the reference drug AZA (IC_{50}=115.1 nM). The compound **TP1** having phenyl ring was found the most potent with IC_{50}=33.0 nM. Introduction of other substituents rather than hydrogen such as methyl, methoxy, polimethoxy, halogens, trifluoromethyl on various positions of phenyl ring and replacement of phenyl by thiophen reduced the inhibition effects of the compounds on hCA II compared with compound **TP1**.

It could be seen from Table 1 that the compounds inhibited AChE with IC_{50} values in the range of 61.6-141.3 nM. Among the series, the compound **TP7** bearing triflоromethyl group at *para* position of phenyl ring was considered the most potent compound with IC_{50}=61.6 nM

among others. Substitution of methyl and triflоromethyl groups at para position of phenyl ring in the compounds **TP2** and **TP7**, or replacement of phenyl by thiophen increased the inhibition effects of the compounds compared with **TP1** and reference drug TAC. However, AChE inhibitory activity decreased by replacing the hydrogen at para position of phenyl with methoxy, polimethoxy and halogen.

5. CONCLUSIONS

4-[5-Aryl-3-(thiophen-2-yl)-4,5-dihydro-1*H*-pyrazol-1-yl] benzenesulfonamide derivatives **TP1-10** were synthesized and biological activities were evaluated towards AChE, hCA I and hCA II enzymes. The compounds were found to have inhibitory activities at nanomolar concentrations against AChE, hCA I, and hCA II isoenzymes. Electronic structure calculations and molecular docking studies were also performed to enlighten inhibition mechanism and to support experimental findings. The experimental and computational findings obtained in the present study might be useful in the design of novel inhibitors against hCA I, hCA II, and AChE.

ACKNOWLEDGEMENTS

The authors thank to Ataturk University BAP office for the financial supports, Ataturk University, Faculty of Science, Department of Chemistry for NMRs, and Anadolu University, Faculty of Pharmacy, Department of Pharmaceutical Chemistry for HRMS analysis.

DECLARATION OF INTEREST

The authors declare that they have no competing interests.

FIGURE LEGENDS AND TABLES

FIGURE 1 Chemical structures of several CA (a) and AChE (b) inhibitors

SCHEME 1 Synthesis of 4-[5-aryl-3-(thiophen-2-yl)-4,5-dihydro-1*H*-pyrazol-1-yl] benzenesulfonamides derivatives, **TP 1-10**

TABLE 1. Inhibitory effects of the compounds **TP 1-10** on AChE, hCA I and hCA II enzymes

TABLE 2 Docking scores and selected molecular properties of **TP1-10** and standard inhibitors

TABLE 3 Selectivity ratios of **TP1-10** and standard inhibitors

FIGURE 2 2D ligand interaction diagrams of AChE-**TP7** (**a**), CA I-**TP8** (**b**) and CA II-**TP1** (**c**) complexes obtained from Glide SP calculations.

REFERENCES

[1] R.A. Copeland, Methods Biochem Anal. 2005, 46, 1.
[2] C.T. Supuran, Nat Rev Drug Discov. 2008, 7, 168.
[3] C.T. Supuran, A. Scozzafava, Bioorg Med Chem. 2007, 15, 4336.
[4] A. Innocenti, S. Beyza Ozturk Sarikaya, I. Gulcin, C.T. Supuran, Bioorg Med Chem. 2010, 18, 2159.
[5] C.T. Supuran, Bioorg Med Chem Lett. 2010, 20, 3467.
[6] A. D. Fiore, C. Pedone, K. D'Ambrosio, A. Scozzafava, G. De Simone, C.T. Supuran, Bioorg Med Chem Lett. 2006, 16, 437.
[7] H.I. Gul, E. Mete, S.E. Eren, H. Sakagami, C. Yamali, C.T. Supuran, J Enzyme Inhib Med Chem. 2017, 32, 169.
[8] H.W. Querfurth, F.M. LaFerla, N Engl J Med. 2010, 362, 329.
[9] D.S. Geldmacher, Prim Care Companion J Clin Psychiatry. 2007, 9, 113.
[10] N. Guzior, A. Wieckowska, D. Panek, B. Malawska, Curr Med Chem. 2015, 22, 373.
[11] M.S. Shah, S.U. Khan, S.A. Ejaz, S. Afridi, S.U. Rizvi, M. Najam-Ul-Haq, J. Iqbal, Biochem Biophys Res Commun. 2017, 482, 615.
[12] M. Ilies, M.D. Banciu, M.A. Ilies, A. Scozzafava, M.T. Caproiu, C.T. Supuran, J Med Chem. 2002, 45, 504.
[13] G. Ucar, N. Gokhan, A. Yesilada, A.A. Bilgin, Neurosci Lett. 2005,382, 327.
[14] O.D. Can, U.D. Ozkay, Z.A. Kaplancikli, Y. Ozturk, Arch Pharm Res. 2009, 32, 1293.
[15] A. Ozdemir, M.D. Altintop, Z.A. Kaplancikli, O.D. Can, U. Demir Ozkay, G. Turan-Zitouni, Molecules. 2015, 20, 2668.
[16] U. Košak, D. Knez, N. Coquelle, B. Brus, A. Pišlar, X. Brazzolotto, J. Kos, J. Colletier, S. Gobec, F. Nachon, Bioorg Med Chem. 2017, 25, 633.
[17] R. Ulus, B. Z. Kurt, I. Gazioglu, M. Kaya, Bioorg Chem. 2017, 70, 245.
[18] C.T. Supuran, J.Y. Winum, Expert Opin Drug Discov. 2015, 10, 591.
[19] J.Y. Winum, C.T. Supuran, J Enzyme Inhib Med Chem. 2015, 30, 321.
[20] F. Carta, L. Di C. Mannelli, M. Pinard, C. Ghelardini, A. Scozzafava, R. McKenna, C.T. Supuran, Bioorg Med Chem. 2015, 23, 1828.
[21] M. O. Pedrosa, R.M. Duarte da Cruz, J. O. Viana, R.O. Moura, H.M. Ishiki, J.M. Barbosa Filho, M.F. Diniz, M.T. Scotti, L. Scotti, F.J. Bezerra Mendonca, Curr Top Med Chem. 2017, 17, 1044.
[22] H.I. Gul, E. Mete, P. Taslimi, I. Gulcin, C.T. Supuran, J Enzyme Inhib Med Chem. 2017,
32, 189.
[23] H.I. Gul, M. Tugrak, H. Sakagami, P. Taslimi, I. Gulcin, C.T. Supuran, J Enzyme Inhib Med Chem. 2016, 31, 1619.
[24] H.I. Gul, C. Yamali, F. Yesilyurt, H. Sakagami, K. Kucukoglu, I. Gulcin, M. Gul, C.T. Supuran, J Enzyme Inhib Med Chem. 2017, 32, 369.
[25] E. Mete, B. Comez, H. Inci Gul, I. Gulcin, C.T. Supuran, J Enzyme Inhib Med Chem. 2016, 31, 1.
[26] K. Kucukoglu, F. Oral, T. Aydin, C. Yamali, O. Algul, H. Sakagami, I. Gulcin, C.T. Supuran, H.I. Gul, J Enzyme Inhib Med Chem. 2016, 31, 20.
[27] C. Yamali, H.I. Gul, H. Sakagami, C.T. Supuran, J Enzyme Inhib Med Chem. 2016, 31 125.
[28] M. Tugrak, C. Yamali, H. Sakagami, H.I. Gul, J Enzyme Inhib Med Chem. 2016, 31 818.
[29] C. Kharbanda, M. S. Alam, H. Hamid, K. Javed, S. Shafi, P. Alam, M. A. Q. Pasha, A. Dhulap, S. Bano, S. Nazreen, Y. Ali, S. Haider, Bioorg Med Chem Lett. 2014, 24, 5298.

[30] K. R. A. Abdellatif, E. K. A. Abdelall, W. A. A. Fadaly, G. M. Kamel, Bioorg Med Chem Lett.
2016, 26, 406.
[31] F. Ozbey, P. Taslimi, I. Gulcin, A. Maras, S. Goksu, C.T. Supuran, J Enzyme Inhib Med Chem. 2016, 31, 79.
[32] P. Taslimi, I. Gulcin, N. Oztaskin, Y. Cetinkaya, S. Goksu, S.H. Alwasel, C.T. Supuran, J Enzyme Inhib Med Chem. 2016, 31, 603.
[33] J.A. Verpoorte, S. Mehta, J.T. Edsall, J Biol Chem. 1967, 242, 4221.
[34] M.M. Bradford, Anal Biochem. 1976, 72, 248.
[35] G.L. Ellman, K.D. Courtney, V. Andres, Jr., R.M. Feather-Stone, Biochem Pharmacol. 1967, 7, 88.
[36] I. Gulcin, A. Scozzafava, C.T. Supuran, Z. Koksal, F. Turkan, S. Cetinkaya, Z. Bingol, Z. Huyut, S.H. Alwasel, J Enzyme Inhib Med Chem. 2016, 31, 1698.
[37] D.O. Ozgun, C. Yamali, H.I. Gul, P. Taslimi, I. Gulcin, T. Yanik, C.T. Supuran, J Enzyme Inhib Med Chem. 2016, 31, 1498.
[38] A. Sujayev, E. Garibov, P. Taslimi, I. Gulcin, S. Gojayeva, V. Farzaliyev, S.H. Alwasel, C.T. Supuran, J Enzyme Inhib Med Chem. 2016, 31, 1531.
[39] E. Harder, W. Damm, J. Maple, C. Wu, M. Reboul, J.Y. Xiang, L. Wang, D. Lupyan, M.K. Dahlgren, J.L. Knight, J.W. Kaus, D.S. Cerutti, G. Krilov, W.L. Jorgensen, R. Abel, R.A. Friesner, J Chem Theory Comput. 2016, 12, 281.
[40] G.M. Sastry, M. Adzhigirey, T. Day, R. Annabhimoju, W. Sherman, J Comput Aided Mol Des. 2013, 27, 221.
[41] R.A. Friesner, J.L. Banks, R.B. Murphy, T.A. Halgren, J.J. Klicic, D.T. Mainz, M.P. Repasky, E.H. Knoll, M. Shelley, J.K. Perry, D.E. Shaw, P. Francis, P.S. Shenkin, J Med Chem. 2004, 47, 1739.
[42] T.A. Halgren, R.B. Murphy, R.A. Friesner, H.S. Beard, L.L. Frye, W.T. Pollard, J.L. Banks, J Med Chem. 2004, 47, 1750.
[43] C.A. Lipinski, Lombardo, F., Dominy, B. W. and Feeney, P. J. , Adv Drug Delivery Rev. 1997, 23, 3.
[44] D.F. Veber, S.R. Johnson, H.Y. Cheng, B.R. Smith, K.W. Ward, K.D. Kopple, J Med Chem. 2002, 45, 2615.
[45] H. Sugimoto, Y. Yamanishi, Y. Iimura, Y. Kawakami, Curr Med Chem. 2000, 7, 303.
[46] A. Ece, B. Pejin, J Enzyme Inhib Med Chem. 2015, 30, 528.
[47] D. Jacquemin, E.A. Perpete, I. Ciofini, C. Adamo, R. Valero, Y. Zhao, D.G. Truhlar, J Chem Theory Comput. 2010, 6, 2071.
[48] N.M. Mascarenhas, N. Ghoshal, Eur J Med Chem. 2008, 43, 2807.
[49] F. Sevin, A. Ece, Med Chem Res. 2013, 22, 5832
[50] Y. Sinhg, S. Srivastava, R. Tripathi, Y. Jain, Int J Pharma Sci and Res. 2015, 6, 939.

TABLE 1 Inhibitory effects of the compounds **TP 1-10** on AChE, hCA I and hCA II enzymes

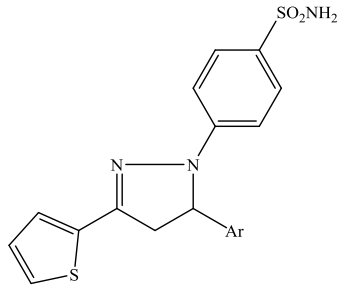

		IC_{50} (nM)						K_I (nM)		
Compound	**Ar**	**hCA I**	**r^2**	**hCA II**	**r^2**	**AChE**	**r^2**	**hCA I**	**hCA II**	**AChE**
TP1	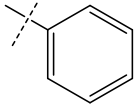	34.7	0.9853	33.0	0.9753	105.4	0.9739	27.8±4.7	40.1±11.1	54.6±1.8
TP2	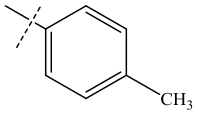	30.1	0.9847	43.3	0.9693	80.1	0.9632	24.8±1.8	42.5±5.7	22.7±10.3
TP3	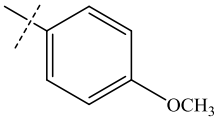	36.5	0.9838	42.1	0.9595	140.0	0.9453	33.1±4.4	62.7±24.7	70.7±22.9
TP4	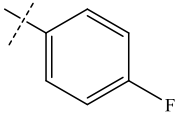	40.8	0.9920	36.5	0.9985	126.3	0.9585	38.0±11.3	38.5±3.8	43.9±20.4

TP5	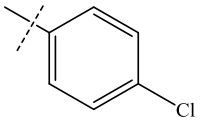	34.5	0.9765	57.8	0.9803	141.3	0.9864	34.3±4.3	65.3±16.7	56.1±22.7
TP6	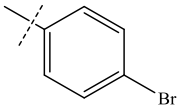	27.7	0.9770	38.5	0.9685	104.8	0.9666	25.6±3.9	37.3±9.0	80.6±37.7
TP7	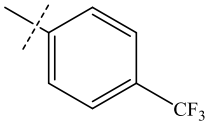	32.8	0.9830	40.5	0.9432	61.6	0.9787	30.1±5.1	55.2±15.6	28.8±9.2
TP8	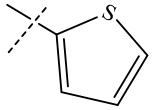	25.7	0.9924	53.3	0.9938	69.7	0.9633	24.2±4.6	44.7±8.9	34.3±15.3
TP9	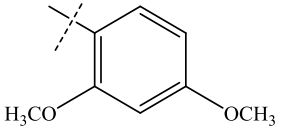	45.8	0.9688	46.2	0.9643	116.2	0.9850	49.8±12.8	49.4±9.3	52.1±21.4
TP10	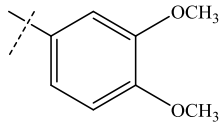	40.5	0.9634	42.2	0.9554	132.6	0.9836	44.8±11.3	43.1±9.9	109.1±27.0
AZA		297.1	0.9889	115.1	0.9719	-	-	282.1±19.71	103.6±27.6	-
TAC		-	-	-	-	115.6	0.9862	-	-	66.5±13.8

TABLE 2 Docking scores and selected molecular properties of **TP1-10** and standart inhibitors

Compound	DScore (kcal/mol)			QPlogPo/w[a]	EHOMO[b] (eV)	Dipole Moment μ (D)[b]	PSA[c] Å^2	%Human Oral Absorption[d]	Rule of Five
	AChE	CA I	CA II						
TP1	-8.50	-6.46	-5.50	3.65	-4.92	7.41	80.65	95.31	+
TP2	-8.92	-6.73	-4.93	3.92	-4.87	7.28	80.09	100.00	+
TP3	-8.88	-6.93	-4.96	3.72	-4.87	7.34	88.45	96.60	+
TP4	-8.89	-6.14	-5.26	3.89	-5.00	7.98	78.40	96.34	+
TP5	-8.69	-6.84	-5.01	4.05	-5.01	8.00	81.03	100.00	+
TP6	-8.61	-6.78	-4.79	4.14	-5.01	7.94	81.14	100.00	+
TP7	-9.39	-6.81	-4.62	4.50	-5.12	9.10	81.14	100.00	+
TP8	-8.72	-6.34	-5.44	3.55	-4.95	7.40	80.21	94.15	+
TP9	-8.70	-6.70	-5.11	3.75	-4.70	6.70	99.10	96.22	+
TP10	-9.17	-6.35	-5.02	3.74	-4.83	7.41	95.23	95.75	+
TAC	-8.85			2.59	-5.13	3.53	34.25	100.00	+
AZA		-6.33	-7.16						

[a] Logarithm of the partition coefficient of the compound between n-octanol and water (recommended value <5)
[b] Calculated at M06-L/6-31+G(d,p)//AM1 level with Spartan '16 parallel suite.
[c] Polar surface area (recommended value ≤ 140Å^2)[45]
[d] Percentage of human oral absorption (<25% is weak and >80% is strong).

TABLE 3 Selectivity ratios of **TP1-10** and standard inhibitors

	K_I (nM)			SR	PSR1	PSR2	PSR3
Compound	**hCA I**	**hCA II**	**AChE**	**hCA II/hCA I**	**hCA I**	**hCA II**	**AChE**
TP1	27.808±4.668	40.142±11.06	54.620±1.821	1.4	10.1	2.6	1.2
TP2	24.771±1.831	42.538±5.660	22.713±10.33	1.7	11.4	2.4	2.9
TP3	33.137±4.428	62.727±24.68	70.710±22.95	1.9	8.5	1.7	0.9
TP4	38.014±11.32	38.470±3.756	43.885±20.42	1.0	7.4	2.7	1.5
TP5	34.254±4.274	65.302±16.56	56.105±22.70	1.9	8.2	1.6	1.2
TP6	25.583±3.984	37.314±9.003	80.580±37.67	1.5	11.0	2.8	0.8
TP7	30.099±5.085	55.181±15.61	28.805±9.211	1.8	9.4	1.9	2.3
TP8	24.181±4.550	44.704±8.925	34.301±15.25	1.8	11.7	2.3	1.9
TP9	49.812±12.80	49.426±9.305	52.070±21.42	1.0	5.7	2.1	1.3
TP10	44.788±11.33	43.138±9.897	109.05±26.95	0.9	6.3	2.4	0.6
AZA*	282.090±19.71	103.60±27.60	-	0.4	-	-	-
TAC**	-	-	66.521±13.76	-	-	-	-

Selectivity Ratio (SR) value reflects the selectivity of a compound towards hCA I or II isoenzymes. The SR values were calculated by dividing Ki value of the certain compounds to hCA II or hCA I. Potency Selectivity Ratios (PSR1 and PSR2) of a compound towards hCA I and II were calculated. PSR1 values were produced by dividing Ki value of AZA (282.090 nM) to Ki value of a certain compound towards hCA I. PSR2 values were produced by dividing Ki value of AZA (103.60 nM) to Ki value of a certain compound towards hCA II. In addition, PSR3 values of the compound towards AChE were calculated. PSR3 values were produced by dividing Ki value of TAC (66.521 nM) to Ki value of a certain compound towards AChE. Data were presented in Table 3.

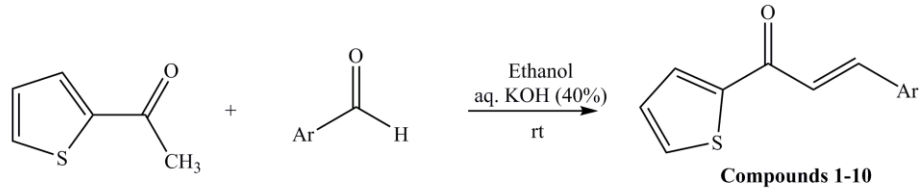

Compounds 1-10

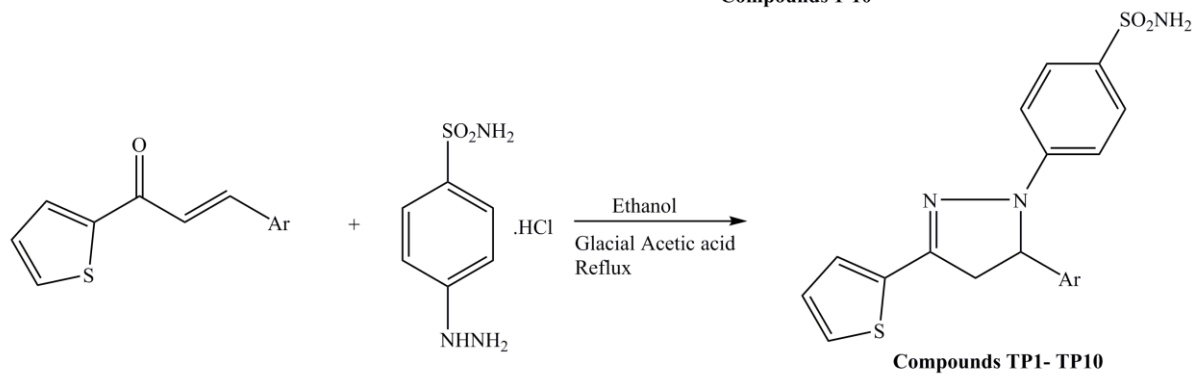

Compounds TP1- TP10

Ar: C_6H_5 for 1, TP1; 4-$CH_3C_6H_4$ for 2, TP2; 4-$CH_3OC_6H_4$ for 3, TP3; 4-FC_6H_4 for 4, TP4; 4-ClC_6H_4 for 5, TP5; 4-BrC_6H_4 for 6, TP6; 4-$CF_3C_6H_4$ for 7, TP7; C_4H_3S(2-yl) for 8, TP8; 2,4-$(CH_3O)_2C_6H_3$ for 9, TP9; 3,4-$(CH_3O)_2C_6H_3$ for 10, TP10.

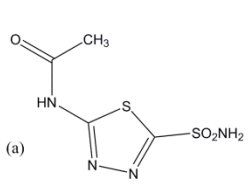

(a) Acetazolamide

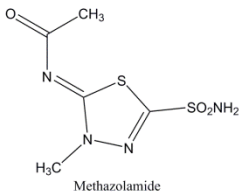

Methazolamide

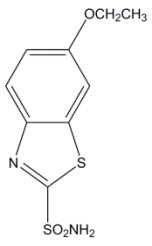

Ethoxzolamide

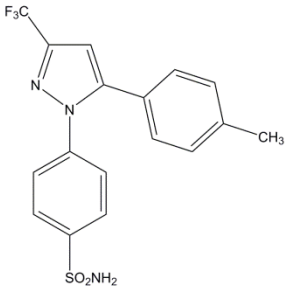

Celecoxib

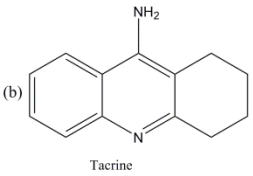

(b) Tacrine

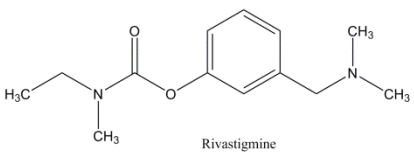

Rivastigmine

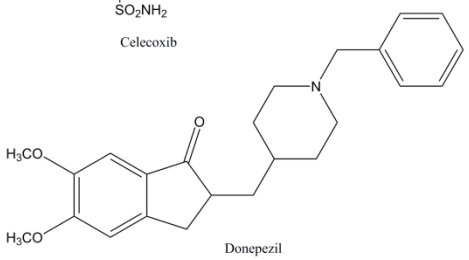

Donepezil